International Journal of Computational and Theoretical Chemistry
2023; 11(1): 19-25
http://www.sciencepublishinggroup.com/j/ijctc
doi: 10.11648/j.ijctc.20231101.12
ISSN: 2376-7286 (Print); ISSN: 2376-7308 (Online)

An Explanation of the Catalpic Acid Low Proportion Through a Theoretical Analysis Performed on the Ricinodendron Heudeulotii

Boka Robert N'Guessan[1], Akpa Eugène Essoh[1], Diakaridja Nikiéma[1], Koua Oi Koua[1], Zéphirin Mouloungui[2], El Hadji Sawaliho Bamba[1, *]

[1]Laboratory of Constitution and Reaction of Matter, Unity of Formation and Research Science of Structure Matter and Technology, University Félix Houphouet-Boigny, Abidjan, Côte d'Ivoire

[2]Laboratory of Agro-Industrial Chemistry, National Polytechnic Institute-National Higher School of Engineers in Chemical and Technological Arts, Toulouse, France

Email address:

nguessanbr@yahoo.fr (Boka Robert N'Guessan), essohakpaeugene@gmail.com (Akpa Eugène Essoh), nikiema1978@gmail.com (Diakaridja Nikiéma), kouaoikoua@yahoo.fr (Koua Oi Koua), zmouloungui@yahoo.fr (Zéphirin Mouloungui) bambaelhadjisawaliho@yahoo.ca (El Hadji Sawaliho Bamba)

[*]Corresponding author

To cite this article:

Boka Robert N'Guessan, Akpa Eugène Essoh, Diakaridja Nikiéma, Koua Oi Koua, Zéphirin Mouloungui, El Hadji Sawaliho Bamba. An Explanation of the Catalpic Acid Low Proportion Through a Theoretical Analysis Performed on the Ricinodendron Heudeulotii. *International Journal of Computational and Theoretical Chemistry*. Vol.11, No. 1, 2023, pp. 19-25. doi: 10.11648/j.ijctc.20231101.12

Received: September 21, 2023; **Accepted**: October 13, 2023; **Published**: October 30, 2023

Abstract: This research focuses on the photochemical activities of Ricinodendron heudeulotii (AKPI) oil, a fatty acid. In general, the latter, a bioactive organic compound, is employed to fight the atherosclerosis, the hypertension, the obesity, or the cancer. Ricinodendron heudeulotii oil contains mainly α-eleostearic acid C18:3c,t,t. This is characterized by its absorbance in ultraviolet or fluorescent light. It can isomerize into β-eleostearic acid C18:3t,t,t and catalpic acid C18:3t,t,c upon exposure to sunlight. The second compound is non-existent in those of certain plants containing the other two. In AKPI oil, it is in the minority. This work aims to explain the basis of its low proportion. The resources of theoretical chemistry were employed. The HF and DFT computations were carried out with the Gaussian09 software. DFT was combined with the B3LYP functional and the 6-311G, 6-311G (d, p), 6-311++G (d, p) basis sets to generate the geometries and calculate the isomer energies. The transition states were determined at the DFT level linked to the same functional and 6–311++G(d, p) base sets. They were carried out according to QST2 protocols. In addition, the low proportion of catalpic acid C18:3t,t,c was explained. It was founded on the recurring instability of α-eleostearic acid C18:3c,t,t compared to β-eleostearic acid C18:3t,t,t. Furthermore, the kinetic process of the first compound's conversion to the second was established.

Keywords: Ricinodendron Heudeulotii Kernel (AKPI), Linoleic Fatty Acid, Photoisomerization, Quantum Calculations

1. Introduction

Dietary lipids come from the animal and plant kingdom. Fatty acids are their main components. They are classified into saturated and unsaturated groups. The latter are monounsaturated or polyunsaturated. Some linoleic and linolenic forms are bioactive molecules; they fought against atherosclerosis and high blood pressure. Their anti-inflammatory and anti-tumor characteristics are very beneficial to human health [1–5]. Ricinodendron heudelotii is an extremely prized foodstuff for these nutritional qualities. These are related to its oil chemical composition and its specific aroma. The insect proliferation is combated by its bioactive constituents [6]. The α-eleostearic acid C18:3c,t,t or 9Z, 11E, 13E, octadecatrienoic acid is its main component. The activities of phospholipases on lipids esterified with

these fatty acids are labelled by its spectrophotometric properties. [7]. According to [8, 9], the transformation of α-eleostearic acid C18:3c,t,t into its conformers β-eleostearic C18:3t,t,t and catalpic C18:3t,t,c is ensured. These changes are highlighted by experiments [10]. The major component of the ricinodendron heudeulotii crude oil is represented by the α-eleostearic acid C18:3c,t,t [11, 12]. The α-eleostearic acid C18:3c,t,t has decreased over time while that of β-eleostearic acid C18:3t,t,t has increased. The second constituent proportion is medium. That of catalpic acid C18:3t,t,c is very low, or even non-existent as in tung [13], flax [14] and soybean oils [15]. Their ratios are varied. However, their basis is not specified. In particular, the foundation of the catalpic C18:3t,t,c acid modest percentage is not justified. The action of enzymes cannot be explained by it. Here, the conversion of α-eleostearic acid C18:3c,t,t is identified. The proportion of the acids related to its metabolism is provided. The theoretical methods are employed for this purpose. Their HF and DFT levels are implemented [16-18]. The density functional B3LYP for the latter has been exploited with the bases of functions such as 6–311 G, 6–311 G (d, p), 6–311++G (d, p). The conversion of α-eleostearic C18:3c,t,t acid into β-eleostearic C18:3t,t,t acid and catalpic C18:3t,t,c acid is demonstrated. The low proportion or the non-existence of the hindmost in the Ricinodendron heudeulotii oil in certain dried fruits is justified.

2. Material and Methods

The geometries of α-eleostearic acid C18:3c,t,t, β-eleostearic acid C18:3t,t,t and catalpic acid C18:3t,t,c were optimized from standard geometrical parameters. The cis and trans-carbon configurations were respected in the Z-matrix constructions by GaussView06. HF and DFT calculations were performed by Gaussian09 software [19]. The density functional B3LYP at the DFT level was utilized for its popularity and quality of results. It associates the set of 6–311G, 6–311G(d,p), 6–311++G(d,p) bases. The transition states (TS) related to photoisomer conversion were determined at DFT degrees by the B3LYP/6–311++G(d, p) functional. They were carried out by QST2 protocols using two optimized structures. All geometry adjustments were verified by vibrational frequency calculations.

3. Results and Discussion

The relative stability of the photoisomers was evaluated by the electronic energies. The following section details their differences.

3.1. Energy Parameters of the Photoisomers

The three photoisomers are isoelectronic molecules. Their optimization structures at the DFT/B3LYP/6-311++G(d,p) level of theory are shown in Figure 1.

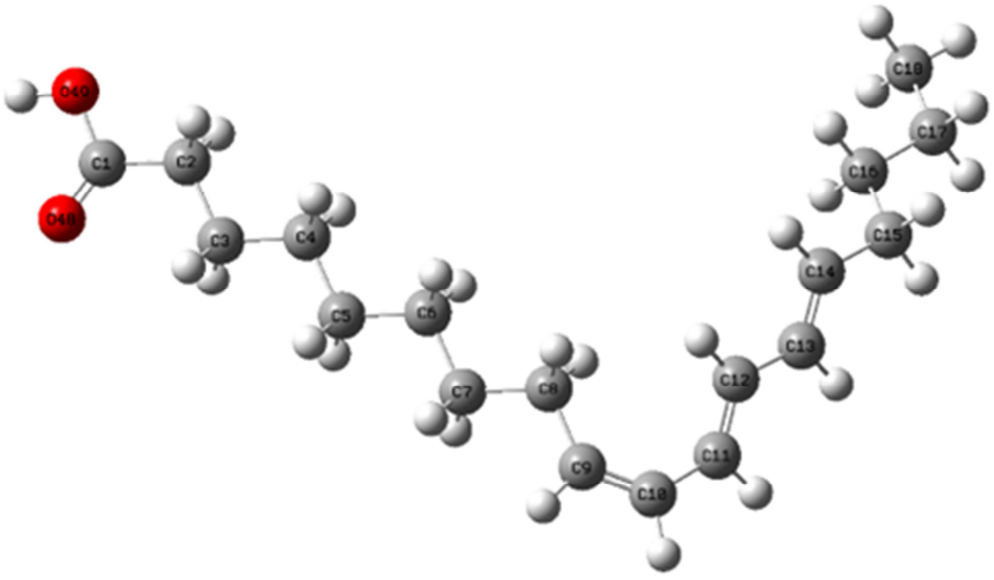

α-eleostearic C18:3c,t,t acid

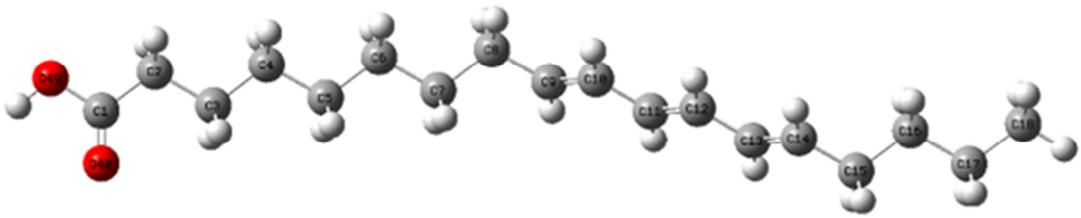

β-eleostearic C18:3t,t,t acid

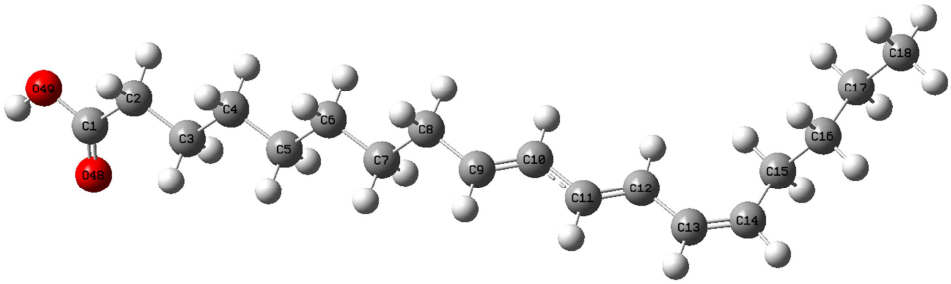

Catalpic C18:3t,t,c acid

Figure 1. *Molecular Structures of α-eleostearic C18: 3c, t, t acid and its Photoisomers.*

A linear appearance to the β-eleostearic acid C18:3t,t,t was given by the transformation from the cis to trans-of C9. A curved one to the catalpic acid is obtained with the changes from the C13 trans-configuration of carbon to the cis configuration. This curvature was less pronounced compared to that of the α-eleostearic acid C18:3c,t,t. The energy values of these molecular systems after the geometry optimizations allowed them to be classified by their stability. This property is mentioned in the following part.

Table 1. *Gaps ΔE1, ΔE2 and ΔE3 of Electronic Energies Between the α-eleostearic acid C18:3c,t,t, the β-eleostearic acid C18:3t,t,t and the catalpic acid C18:3t,t,c in kcal/mol.*

Computation level	**HF**	**DFT/B3LYP**		
Basis set	**6-31G**	**6-311G**	**6-311G(d, p)**	**6-311++G(d, p)**
ΔE_1	5.020	5.020	5.020	5.648
ΔE_2	3.137	3.765	3.765	4.393
ΔE_3	1.883	1.255	1.255	1.255

3.1.1. Stability of the Photoisomers

Table 1 gathers the energetic gaps between the photo-isomers. The differences between their electronic energies after the geometrical optimizations were related to the latter. ΔE1, ΔE2 and ΔE3 respectively were those denoted between the α-eleostearic acids C18:3c,t,t and the β-eleostearic acids C18:3t,t,t. Then, they are referred to those between the first cited and catalpic acids C18:3t,t,c and finally between the second one and catalpic acids C18:3t,t,c. These results indicated that ΔE1> ΔE2> ΔE3 for both levels of calculation. In the B3LYP/6-311++G(d,p) bases at the DFT degree, the electronic energy of the fatty acids was such that: E(C18:3c,t,t)> E(C18:3t,t,c)> E(C18:3t,t,t). They were respectively worth in atomic units (-854,670) (-854,677) and (-854,679).

The order of the energies remained the same in the other basis sets and at all levels of computation. The results are refined with the B3LYP/6-311G(d,p) and B3LYP/6-311++G(d,p) bases. The polarization and diffuse functions were contributed to a better description of the photoisomers energy levels. The energies of the α-eleostearic acid C18:3c,t,t (6902 kcal/mol), the β-eleostearic acid C18:3t,t,t or the catalpic acid C18:3t,t,c (7530 kcal/mol) were stabilized by the polarization functions with the B3LYP/6-311G(d,p) calculations. The latter were found to be important. The ΔE1 gaps stayed the same (5,020 kcal/mol) for HF/6-31G and for B3LYP/6-311G and B3LYP/6-311G(d, p) at the DFT level. They increased to 5,648 kcal/mol for B3LYP/6-311++G(d, p). The ΔE2 was also identical for the first two basis sets (3,765 kcal/mol) at the same degree. But it was lower than that of the largest ones (4,393 kcal/mol). The ΔE3 does not change for the calculations at the DFT level (1,255 kcal/mol). It was equalled to 1,883 kcal/mol in HF/6-31G.

The stability energies of the photoisomers were ranked from the most to the least robust in the following order: the β-eleostearic acid C18:3t,t,t, the catalpic acid C18:3t,t,c and the α-eleostearic acid C18:3c,t,t. The α-eleostearic acid C18:3c,t,t was converted to the β-eleostearic acid C18:3t,t,t or the catalpic acid C18:3t,t,c; this last was transformed to its β-eleostearic C18:3t,t,t isomer. The mutation possibilities are discussed with the activation energies in the next section.

3.1.2. Transition State Between Photoisomers

The electronic energies of the photoisomers were well evaluated by the largest basis set at DFT level. Those of the transition states are determined with them by the QST2 protocol. Their activation energies are summarized in Table 2. Their energy profiles between the photoisomers are shown in Figure 2. Their energy gaps with respect to them are illustrated. They were closely related to the kinetics of the transformation.

Table 2. *Energy Levels in the Transition State (ua) and Activation Energy (kcal/mol) of the Transformations Calculated at the DFT Level by B3LYP/6-311++G(d, p).*

Transitions states (TS)	**Electronic energies (ua)**	**Activation barrier E_A (kcal/mol)**
TS_1 (CTT-TTT)	-854.665367	3,138
TS_2 (CTT-TTC)	-854,664007	3,765
TS_3 (TTT-TTC)	-854,674798	2,637

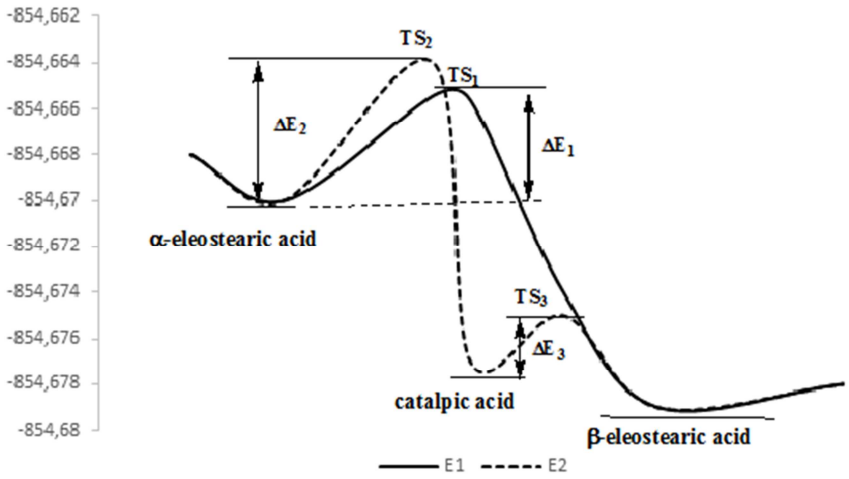

Figure 2. *Reaction Paths, Transition States and Activation Energies Associated with Photoisomer Conversions of α-eleostearic acid.*

The photo-conversion of the α-eleostearic acid C18:3c,t,t to the β-eleostearic acid C18:3t,t,t. was described by the pathway E1 in a solid line. That of its transformation into the β-eleostearic acid C18:3t,t,t via catalpic acid C18:3t,t,c was corresponded to the E2 in a dotted line. The α-eleostearic acid C18:3c,t,t was the highest. It can be converted into the other two. An activation energy of 3.138 kcal/mol was required for the change to β-eleostearic acid C18:3t,t,t. It was lower than that of its mutation to the catalpic acid C18:3t,t,c; It equalled to 3.765 kcal/mol. The first transition was the most favourable. However, the second was likely remained; the activation energy between the two transformations was deviated by only 0.627 kcal/mol. In addition, the energy level of the catalpic acid C18:3t,t,c was intermediate between those of the α-eleostearic acid C18:3c,t,t and the β-eleostearic acid C18:3t,t,t. The latter transition corresponded to an activation energy of 2.637 kcal/mol. It was much more labile than the other two. Moreover, it could only occur after the first step disadvantaged the activation barrier of 3.765 kcal/mol. A total energy of 6.402 kcal/mol versus 3.138 kcal/mol was required for the dotted pathway to convert α-eleostearic acid C18:3c,t,t to β-eleostearic acid C18:3t,t,t. The experimental observations were corroborated; the exposure to daylight of crude petroleum had simulated those obtained using the Sun Test. These results are below illustrated in Figure 3. The tracing of the fatty acid profiles was carried out following the different vegetable oil samples subjected to UV light for 4h, 8h and 12h.

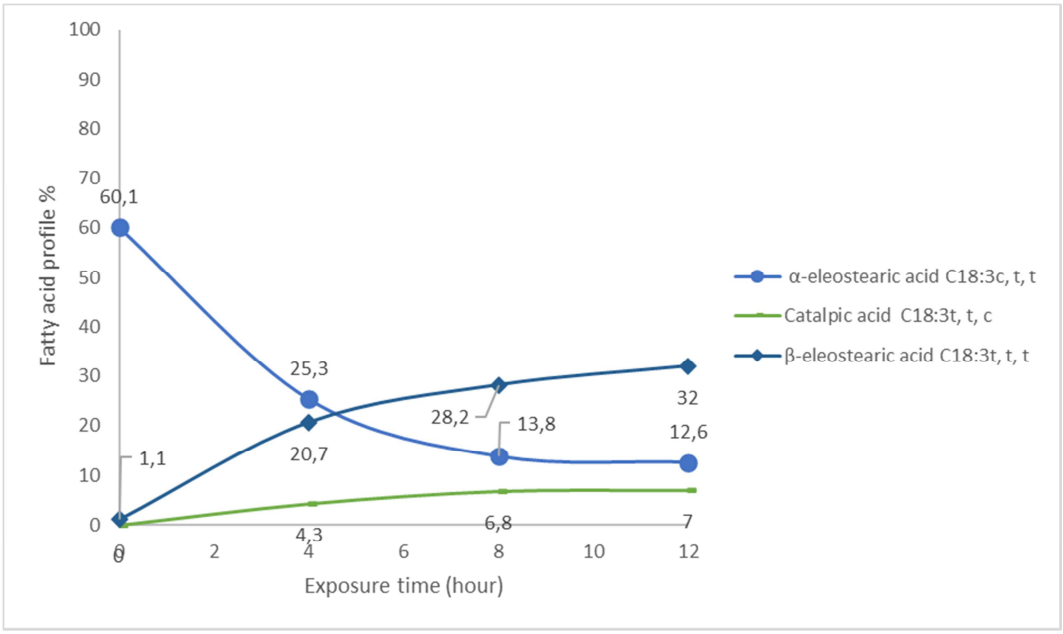

Figure 3. *Evolution of fatty acid profiles of crude oil modified by UV Sun Test.*

The downward trend in α-eleostearic acid C18:3c,t,t content was evident. The fall in concentration was strong at 4h of exposure to UV. It was carried out in favour of those of the β-eleostearic acid C18:3t,t,t and the catalpic acid C18:3t,t,c. Then, its accumulation was stabilized after 8h and 12h. A proportion of 46.3% of the α-eleostearic acid C18:3c,t,t was

decreased. A rise of 27.1% in β-eleostearic acid C18:3t,t,t and 6.8% in catalpic acid C18:3t,t,c was achieved. More, 63% of the α-eleostearic acid C18:3c,t,t were isomerized to 51.4% of the β-eleostearic acid C18:3t,t,t and to 11.6% of the catalpic acid C18:3t,t,c. This last conversion was resulted by the subjecting crude oil to UV for 12 hours. The catalpic acid C18:3t,t,c was remained in a tiny proportion while that of the β-eleostearic acid C18:3t,t,t was jumped more strongly. This rapid increase was corresponded to the first kinetic process that was used very little activation energy. The transformation of the β-eleostearic acid C18:3t,t,t was impossible; it would lead to a high-energy structure. The C18:3t,t,c catalpic acid presence was explained by the probability of the second mechanism; the last was resulted to the small energy difference between the two transition states of 0.627 kcal/mol. The activation energy from the catalpic acid C18:3t,t,c to the β-eleostearic acid C18:3t,t,t was much minute compared to that of the other two. The transformation of the entire catalpic acid C18:3t,t,c was favoured. Nevertheless, the proximity of their energy levels was reflected in the low ΔE3 values. The lifetime of the C18:3t,t,c catalpic acid was extended; this photoisomer was artificially accumulated on an energetically disadvantaged reaction pathway. Exposure to UV rays from the sun for three to six months resulted in the low proportion production of catalpic acid C18:3t,t,c in the almond oil extracts of Ricinodendron heudeulotii. The profiles of the three fatty acids after the second period are shown in Figure 4.

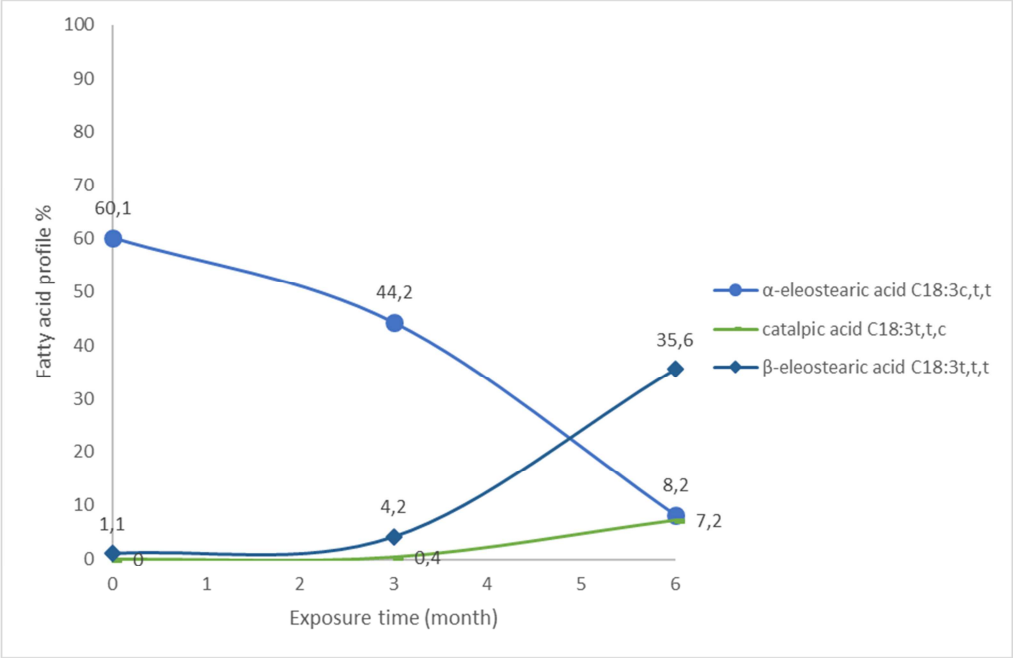

Figure 4. *Ricinodendron Heudelotii Crude Oil Fatty Acid Profiles Modified by Sunlight.*

The results showed that the α-eleostearic acid C18:3c,t,t decreases by 51.9%; this decrease in its concentration led to an increase of 7.2%, for the catalpic acid C18:3t,t,c and 34.5% for the β-eleostearic acid C18:3t,t,t. The exposure of the oil to sunlight conducted to the α-eleostearic acid C18:3c,t,t. The last photoisomer was converted to the β-eleostearic acid C18:3t,t,t and the catalpic acid C18:3t,t,c. This natural process of the α-eleostearic acid C18:3c,t,t transformation agrees with the theoretical findings. The proportion of the catalpic acid C18:3t,t,c was small while that of the β-eleostearic acid C18:3t,t,t increases more rapidly. The geometrical parameters mark the structural differences between the photoisomers. The following section discusses these aspects.

3.2. Geometrical Parameters of Photoisomers

The geometrical optimizations provided access to the bond lengths and bindings and dihedral angles. The parameters calculated at the HF or DFT level of theory are grouped in Table 3.

The absence of experimental data in the literature did not allow comparisons with theoretical ones. Nevertheless, Data on similar molecular structures was an indication on the accuracy of the computational results. The bond lengths of the three photoisomers were approximately identical at the HF level. The double cross-link of 1,314 Å was different from the single ones of 1.51 Å. This result was the same with the other three basis sets used in DFT. The diffuse and polarization functions did not make significant changes to the bond lengths. However, variations in linkage angles were noticeable. Those associated with double bindings were oscillated between 125° (the α-eleostearic acid C18:3c,t,t) and 128.5° (the catalpic acid C18:3t,t,c) for HF. Those of β-eleostearic acid C18:3t,t,t remained on average at 125°. At the DFT level, they were unmodified while those of the first two acids mentioned fluctuated from 124° to 129°. For these, the angles centred on the C9, C10 and C11 atoms were high (higher than 127°) while those on C12, C13 and C14 were lower (around 124°). All others were near 124° for the β-eleostearic acid C18:3t,t,t.

The dipole moments were impacted.

The dipole moments were respectively equalled to 2.22 D, 1.75 D, and 1.66 D for the α-eleostearic acid C18:3c,t,t, the β-eleostearic acid C18:3t,t,t and the catalpic C18:3t,t,c in HF. Their variations were not enough to distinguish them by the dipolmetry method. The lowest dipole moment was that of the β-eleostearic acid C18:3t,t,t according to the DFT findings. Different characteristics were revealed by the Infrared spectroscopy.

Table 3. *Geometrical Parameters and Dipole Moments of Photoisomers at HF Levels.*

Liaisons	HF			DFT								
	6-311G			B3LYP/6-311G			B3LYP/6-311G(d, p)			B3LYP/6-311++G(d, p)		
	AEL-CTT	AEL-TTT	ACA-TTC	AEL-CTT	AEL-TTT	ACA-TTC	AEL-CTT	AEL-TTT	ACA-TTC	AEL-CTT	AEL-TTT	ACA-TTC
C_8-C_9	1.505	1.502	1.504	1.506	1.507	1.503	1.502	1.499	1.499	1.502	1.499	1.499
C_9-C_{10}	1,332	1,330	1,333	1.349	1.503	1.347	1.345	1.343	1.343	1.346	1.344	1.344
C_{10}-C_{11}	1,470	1,459	1,460	1.461	1.450	1.450	1.459	1.447	1.447	1.459	1.448	1.447
C_{11}-C_{12}	1,334	1,335	1,336	1.354	1.354	1.355	1.350	1.350	1.351	1.351	1.351	1.351
C_{12}-C_{13}	1,461	1,459	1.460	1,452	1,450	1,451	1,449	1,447	1,448	1,449	1,448	1,448
C_{13}-C_{14}	1.330	1.330	1,333	1,347	1,347	1,350	1,342	1,343	1,346	1,343	1,344	1,347
C_{14}-C_{15}	1,502	1,502	1,504	1,503	1,503	1,505	1,499	1,499	1,501	1,499	1,499	1,501
μ (D)	2,220	1,747	1,659	2,009	1,442	1,666	1,970	1,362	1,761	2,161	1,497	1,626

3.3. Spectroscopic Parameters

Each of the photoisomers had three double bonds. The frequencies of their elongations are gathered in Table 4. The stretching C=C of the HF calculations were very high compared to the standard experimental values. This level overestimates them. The DFT results had lowered them. The elongations of these three double bonds were combined in the pairs by symmetric and asymmetric modes. Their mixtures at the DFT level by B3LYP/6-311++G(d,p) are summarized in Table 4.

The vibrational frequencies of these elongations were distinct from those of C=O, C-O, C-C and C-H. Those of C=C had characterized the cis and trans configurations of the hydrogen connected to the ethylenic carbons. They were discriminated by three bands between 1635 cm^{-1} and 1705 cm^{-1}. They were of very weak intensities; however, the largest corresponded to the strongest of the three. Those of 1651 cm^{-1} 1647 cm^{-1} and 1637 cm^{-1} were respectively related to the small C=C elongations of α-eleostearic acid C18:3c,t,t; β-eleostearic acid C18:3t,t,t and catalpic acid C18:3t,t,c. They described the combination of two asymmetric modes and another symmetric one as detailed in Table 4. The frequency variation (Δν) was equivalent to the difference between two successive vibrations for a given structure. For α-eleostearic acid C18:3c,t,t, those at 20 cm^{-1} and 27 cm^{-1} resulted from the symmetrical attenuation modes of the two terminal double bonds. They also came from the asymmetric modes located at the centre and end of the chains. The same type of change was explained in the variation of 27 cm^{-1}.

For the β-eleostearic acid C18:3t,t,t, the shift of 40 cm^{-1} was derived to three symmetric vibrational pair combinations. The first two was of very low intensity. The most significant structure was the last one at 1701 cm^{-1}. Its intensity reached 8,694. It corresponded to an asymmetric stretching between the two terminal double bonds. The observation was like the catalpic acid C18:3t,t,c; nevertheless, the intensities of the two previous differ from zero contrary to the case of the β-eleostearic acid C18:3t,t,t. The three isomers of the studied acids were discriminated by infrared spectroscopy.

The asymmetric vibration intensities of the double bonds C9=C10 and C13=C14 were detectable although they were associated with very close frequencies. These appear respectively in 1698 cm^{-1}, 1701 cm^{-1} and 1695 cm^{-1} for the α-eleostearic acid C18:3c,t,t, the β-eleostearic acid C18:3t,t,t and the catalpic acid C18:3t,t,c. This observation is followed by the conclusion.

Table 4. *Elongation Frequencies ν((C=C)) of α-eleostearic acid C18:3c,t,t; β-eleostearic acid C18:3t,t,t and catalpic acid C18:3t,t,c.*

Fatty acids	Frequencies $\nu(cm^{-1})$	Intensities	Variation $\Delta\nu(cm^{-1})$	Assignations
α-eleostearic acid C18:3c,t,t	1651	4.020	-	ν_s(C9=C10, C11=C12)+ν_{as}(C11=C12, C13=C14)+ν_{as}(C9=C10, C13=C14)
		1.740	20	ν_{as}(C9=C10, C11=C12)+ν_{as}(C11=C12, C13=C14)+ν_s(C9=C10, C13=C14)
	1698	7.870	27	ν_{as}(C9=C10, C11=C12)+ν_s(C11=C12, C13=C14)+ν_{as}(C9=C10, C13=C14)
β-eleostearic acid C18:3t,t,t	1647	0.001	-	ν_{as}(C9=C10, C11=C12)+ν_{as}(C11=C12, C13=C14)+ν_s(C9=C10, C13=C14)
	1687	0.051	40	ν_s(C9=C10, C11=C12, C13=C14)
	1701	8,694	14	ν_{as}(C9=C10, C13=C14)
Catalpic acid C18:3t, t, c	1637	3,279	-	ν_{as}(C9=C10, C11=C12)+ν_{as}(C11=C12, C13=C14)+ν_s(C9=C10, C13=C14)
	1682	1,142	45	ν_s(C9=C10, C11=C12, C13=C14)
	1695	7,528	13	ν_{as}(C9=C10, C13=C14)

4. Conclusion

Understanding the dynamics between the α-eleostearic acid C18:3c,t,t, the β-eleostearic acid C18:3t,t,t and the catalpic acid C18:3t,t,c was the focus of this work. This research has established that the photochemical activities reported in AKPI oil upon exposure to sunlight transform its components. The

α-eleostearic acid C18:3c,t,t is represented as the main one. Its isomerization into catalpic acid C18:3t,t,c and β-eleostearic acid C18:3t,t,t obeys the principles of energetic and kinetic stability. The low proportion of the catalpic acid C18:3t,t,c is related to the energetic characteristic of the reaction path. The reason why this constituent remains very minor in the composition of the oil is explained. Its particularity is based on the recurrent instability dynamics of α-eleostearic acid C18:3c,t,t with respect to β-eleostearic acid C18:3t,t,t. Furthermore, the rapid increase in its percentage of β-eleostearic acid C18:3t,t,t proceeds from a kinetic process.

References

[1] Susan Costantini, Fabiola Rusolo, Valentina de Vito, Stefania Moccia, Gianluca Picariello, Francesca Capone... and Maria Grazia Volpe. (2014). Potential anti-inflammatory effects of the hydrophilic fraction of pomegranate (Punica granatum L.) seed oil on breast cancer cell lines. *Molecules (Basel, Switzerland)* (6). DOI: 10.3390/molecules19068644.

[2] Laura den Hartigh. (2019). Conjugated Linoleic Acid Effects on Cancer, Obesity, and Atherosclerosis: A Review of Preclinical and Human Trials With Current Perspectives. *Nutrients* (2). DOI: 10.3390/nu11020370.

[3] Guixiang Zhao, Terry D. Etherton, Keith R. Martin, Sheila G. West, Peter J. Gillies and Penny M. Kris-Etherton. (2004). Dietary alpha-linolenic acid reduces inflammatory and lipid cardiovascular risk factors in hypercholesterolemic men and women. *The Journal of nutrition* (11). DOI: 10.1093/jn/134.11.2991.

[4] A. P. Simopoulos. (2000). Human requirements for N-3 polyunsaturated fatty acids. *Poultry science* (7). DOI: 10.1093/ps/79.7.961.

[5] Tsuyoshi Tsuzuki, Yoshiko Tokuyama, Miki Igarashi and Teruo Miyazawa. (2004). Tumour growth suppression by alpha-eleostearic acid, a linolenic acid isomer with a conjugated triene system, via lipid peroxidation. *Carcinogenesis* (8). DOI: 10.1093/carcin/bgh109.

[6] Tamuno-Boma Odinga, Sammer Yousuf, Muhammad Iqbal Choudhary, Gloria Ihuoma Ndukwe, Prayer Chidi Obinna, Miebaka Beverly Otobo and Caleb Chimuanya Nwokogba. (2023). Bioactive Components, Anti-Dengue, and Insecticidal Potencies of Ricinodendron Heudelotii (Baill). Seed Oil. *International Journal of Medicinal Plants and Natural Products* (1). DOI: 10.20431/2454-7999.0901002.

[7] Stephanie P. B. Caligiuri, Karin Love, Tanja Winter, Joy Gauthier, Carla G. Taylor, Tom Blydt-Hansen … and Harold M. Aukema. (2013). Dietary linoleic acid and α-linolenic acid differentially affect renal oxylipins and phospholipid fatty acids in diet-induced obese rats. *The Journal of nutrition* (9). DOI: 10.3945/jn.113.177360.

[8] Frédéric Beisson, Natalie Ferté, Joannès Nari, Georges Noat, Vincent Arondel and Robert Verger. (1999). Use of naturally fluorescent triacylglycerols from Parinari glaberrimum to detect low lipase activities from Arabidopsis thaliana seedlings. *Journal of Lipid Research* (12). DOI: 10.1016/S0022-2275 (20)32106-4.

[9] Gaëlle Pencreac'h, Jean Graille, Michel Pina … and Robert Verger. (2002). An ultraviolet spectrophotometric assay for measuring lipase activity using long chain triacyglycerols from Aleurites fordii seeds. *Analytical biochemistry* (1). DOI: 10.1006/abio.2001.5427.

[10] H. Ghomdim Nzali, C. Tchiegang, E. Mignolet, C. Turu, Y. Larondelle… and M. Meurens. (2012). Study of Bioconversion of Conjugated Linolenic Acid (CLNA) of Ricinodendron heudelotii (bail). Seed in Male Rats into Conjugated Linoleic Acid (CLA) Using UV-Vis Spectrometry and Gas Chromatography. *Asian Journal of Biochemistry* (4). DOI: 10.3923/ajb.2012.194.205.

[11] Diakaridja Nikiema. Huile native et huile traitée de Ricinodendron heudelotii: biodisponibilité, structure et réactivité chimio-enzymatique des acides gras linoléniques conjugués CLnA — (Alpha et Beta) — éléostéarique. https://oatao.univ-toulouse.fr/28652/.

[12] Diakaridja Nikiema, Zéphirin Mouloungui, Koua oi Koua, Muriel Cerny, Éric Lacroux, Romain Valentin and Adjou Ané. (2019). The effect of dehulling method on the chemical composition of the lipid constituents of the kernels and oils of Ricinodendron heudelotii seeds. *Industrial Crops and Products*, *140*, 111614. DOI: 10.1016/j.indcrop.2019.111614.

[13] Nelson Zornitta, Willian Cézar Nadaleti, Reinaldo Aparecido Bariccatti, Reginaldo Ferreira dos Santos, Rafael Linzmeyer Zornitta and Carlos Eduardo Camargo Nogueira. (2017). <b> Evaluation of the Tung's fruits as a possible source of sustainable energy. *Acta Scientiarum. Technology* (4). DOI: 10.4025/actascitechnol.v39i4.29857.

[14] Somaia Al-Madhagy, Naglaa S. Ashmawy, Ayat Mamdouh, Omayma A. Eldahshan and Mohamed A. Farag. (2023). A comprehensive review of the health benefits of flaxseed oil in relation to its chemical composition and comparison with other omega-3-rich oils. *European journal of medical research* (1). DOI: 10.1186/s40001-023-01203-6.

[15] Tom E. Clemente and Edgar B. Cahoon. (2009). Soybean oil: genetic approaches for modification of functionality and total content. *Plant physiology* (3). DOI: 10.1104/pp.109.146282.

[16] Robert Ghormley Parr. (1980). Density Functional Theory of Atoms and Molecules. Horizons of Quantum Chemistry. Académie Internationale des Sciences moléculaires quantiques/International Academy of Quantum Molecular Science. (3). doi.org/10.1007/978-94-009-9027-2_2.

[17] Douglas Rayner Hartree. (1928). The Wave Mechanics of an Atom with a Non-Coulomb Central Field. Part I. Theory and Methods. *Mathematical Proceedings of the Cambridge Philosophical Society* (1). DOI: 10.1017/S0305004100011919.

[18] Kenichi Fukui and Bernard Pullman. (1979). *Horizons of Quantum Chemistry*: *Proceedings of the Third International Congress of Quantum Chemistry Held at Kyoto, Japan, October 29—November 3, 1979;* Springer International Publishing, 2012. DOI: 10.1007/978-94-009-9027-2.

[19] Michael Frisch, G. W. Trucks, H. B. Schlegel, G. E. Scuseria, M. A. Robb … and D. J. Fox. (2009), Gaussian 09 Revision D. 01. Gaussian, Inc., Wallingford, CT.